Inorganic Chemistry

pubs.acs.org/IC

Article

Bn_2DT3A, a Chelator for ^{68}Ga Positron Emission Tomography: Hydroxide Coordination Increases Biological Stability of $[^{68}Ga][Ga(Bn_2DT3A)(OH)]^-$

Thomas W. Price, Isaline Renard, Timothy J. Prior, Vojtěch Kubíček, David M. Benoit, Stephen J. Archibald, Anne-Marie Seymour, Petr Hermann, and Graeme J. Stasiuk*

Cite This: *Inorg. Chem.* 2022, 61, 17059−17067

Read Online

ACCESS | Metrics & More | Article Recommendations | Supporting Information

ABSTRACT: The chelator $\mathbf{Bn_2DT3A}$ was used to produce a novel ^{68}Ga complex for positron emission tomography (PET). Unusually, this system is stabilized by a coordinated hydroxide in aqueous solutions above pH 5, which confers sufficient stability for it to be used for PET. $\mathbf{Bn_2DT3A}$ complexes Ga^{3+} in a hexadentate manner, forming a *mer-mer* complex with log $K([Ga(\mathbf{Bn_2DT3A})])$ = 18.25. Above pH 5, the hydroxide ion coordinates the Ga^{3+} ion following dissociation of a coordinated amine. $\mathbf{Bn_2DT3A}$ radiolabeling displayed a pH-dependent speciation, with $[^{68}Ga][Ga(\mathbf{Bn_2DT3A})(OH)]^-$ being formed above pH 5 and efficiently radiolabeled at pH 7.4. Surprisingly, $[^{68}Ga][Ga(\mathbf{Bn_2DT3A})(OH)]^-$ was found to show an increased stability *in vitro* (for over 2 h in fetal bovine serum) compared to $[^{68}Ga][Ga(\mathbf{Bn_2DT3A})]$. The biodistribution of $[^{68}Ga][Ga(\mathbf{Bn_2DT3A})(OH)]^-$ in healthy rats showed rapid clearance and excretion *via* the kidneys, with no uptake seen in the lungs or bones.

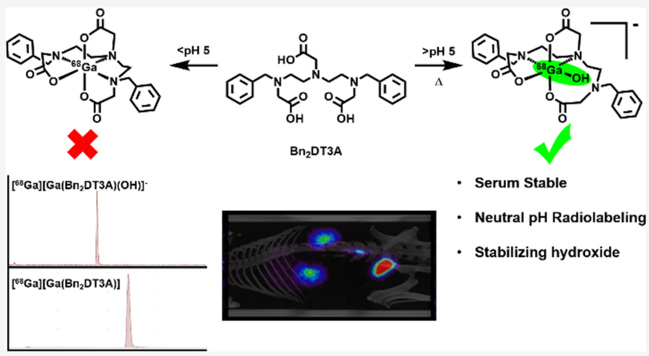

■ INTRODUCTION

Positron emission tomography (PET) is a highly sensitive technique that can be used to image molecular processes.[1] While the resolution is not as high as other imaging modalities (typically in the mm range),[1] the high sensitivity allows for target-specific imaging of cellular receptors using peptides and antibodies.[2]

A range of radioactive nuclei can be used for PET;[2] gallium-68 (^{68}Ga) is a PET isotope that has favorable physical decay properties for diagnostic imaging,[3,4] with a high positron branching ratio (β^+ = 89%) and a half-life ($\tau_{1/2}$ = 67.71 min) suitable for use with small peptide targeting units.[2−4] ^{68}Ga is also available from a radionuclide generator.[4] This is a more accessible route to on-site isotope production than the more conventional cyclotron production, although the activities produced are lower than those achievable by cyclotron production of ^{68}Ga.[5−7]

While weakly coordinated Ga^{3+} salts such as gallium citrate or nitrate have been used in clinical nuclear imaging,[5] to achieve more specific images of disease, ^{68}Ga is typically incorporated into a radiotracer through the use of a chelator.[5,8] These radiotracers have found significant success in recent years, in particular the somatostatin targeting $[^{68}Ga][Ga(\mathbf{DOTATATE})]$, which has been approved for diagnostic imaging of neuroendocrine tumors[9,10] and prostate specific membrane antigen targeting ^{68}Ga probes, which are being utilized clinically for identification of prostate cancer metastases.[11−15]

A range of chelators have been applied to ^{68}Ga complexation;[8,16] the most widely used is the macrocycle 1,4,7,10-tetraazacyclododecane-1,4,7,10-tetraacetic acid (**DOTA**, Figure S1).[5,16] **DOTA** is a versatile chelator, capable of complexing a variety of metals.[5] However, this versatility also means that it is not the ideal chelator for ^{68}Ga.[16] This is reflected in the forcing radiolabeling conditions required for radiochemical yields (RCYs) >95% (elevated temperatures of 80 °C and acidic conditions of pH 4)[17,18] and reduced stability of the resulting complex (80% intact after 2 h incubation in serum).[19] A more suitable macrocyclic chelator, 1,4,7-triazacyclononane-1,4,7-triacetic acid (**NOTA**, Figure S1), demonstrates the improved radiolabeling efficiency (no heating required)[16−18,20] and stability (>98% stable to serum over 2 h)[19,20] that can be obtained by using specifically designed chelators for ^{68}Ga.

Received: June 9, 2022
Published: October 17, 2022

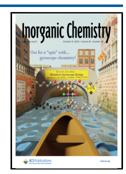

Scheme 1. Synthesis of Bn_2DT3A and Subsequent Complexation of Ga^{3+}. (a) (i) EtOH, Benzaldehyde, Reflux. (ii) $NaBH_4$, 0 °C. (b) MeCN, Na_2CO_3, *tert*-Butyl Bromoacetate, 60 °C. (c) DCM, TFA. 0 °C to RT. (d) H_2O, $GaCl_3$, pH 4, Reflux

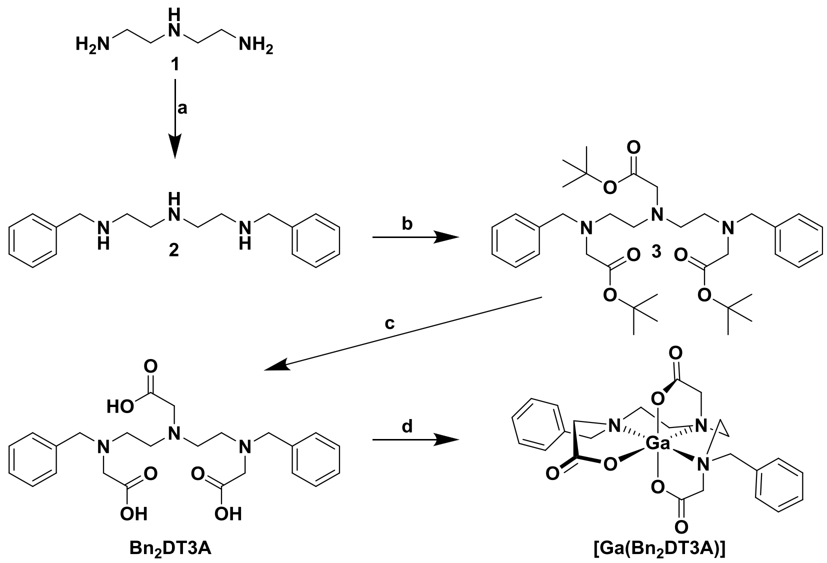

An area of growing interest in the development of chelators for ^{68}Ga is the ability to radiolabel the chelator at higher pH values.[8,21,22] This would allow for a simpler radiolabeling process and for the use of targeting moieties that may degrade under acidic conditions, expanding the breadth of diagnostic agents possible using ^{68}Ga.[22] Some key examples of chelators that have achieved this goal are 4-acetamido-N^1,N^7-bis[(3-hydroxy-1,6-dimethyl-4-oxo-1,4-dihydropyridin-2-yl)methyl]-4-(3-{[(3-hydroxy-1,6-dimethyl-4-oxo-1,4-dihydropyridin-2-yl)methyl]amino}-3-oxopropyl)heptanediamide (**THP**, Figure S1),[23,24] 2,2′-{6-[(1-carboxyethyl)amino]-6-phenyl-1,4-diazepane-1,4-diyl}dipropionic acid (**DATA^{PPh}**, Figure S1),[25] and 2,2′-{ethane-1,2-diylbis[(2-hydroxybenzyl)azanediyl]}diacetic acid (**HBED**, Figure S1).[12,22,26] These chelators have an acyclic or semicyclic design that improves the coordination kinetics.

Substitution of chelators can impact upon the biodistribution of PET radiotracers;[27,28] as such, having a range of suitable chelators will aid in the rapid development of a radiotracer with optimized biodistribution and target uptake. Further development of chelators for ^{68}Ga will also aid in the understanding of the design of systems capable of producing highly stable chelates under mild conditions. This would allow for the radiolabeling of sensitive biomolecules possessing an appropriate biological half-life.

In this manuscript, we report the synthesis of a novel hexadentate acyclic chelator, 2,2′-({[(carboxymethyl)-azanediyl]bis(ethane-2,1-diyl)}bis[benzylazanediyl])-diacetic acid (**Bn_2DT3A**, Scheme 1), characterize its Ga^{3+} complex, and explore the radiolabeling efficiency of this system with ^{68}Ga. **Bn_2DT3A** resembles the well-studied diethylenetriamine-*N*,*N*,*N*′,*N*″,*N*″-pentaacetic acid (**DTPA**, Figure S1) chelator; however, benzyl units have been substituted in place of two of the acetic acid arms. While **DTPA** has been applied to ^{68}Ga complexation, the radiolabeling efficiency was not sufficiently high[29,30] and the resulting complex was unstable under relevant biological conditions.[29,30] A more rigid derivative, 2,2′-{[2-({2-[bis(carboxymethyl)amino]-cyclohexyl}[carboxymethyl]-amino)ethyl]azanediyl}diacetic acid (**CHX-A″-DTPA**, Figure S1), has been demonstrated to produce a stable complex with ^{68}Ga[31,32] and applied to imaging in humans.[32] The substitution of the acetate arms of **DTPA** for benzyl units to give **Bn_2DT3A** results in a chelator with a coordination number that matches the ideal octahedral Ga^{3+} coordination sphere (coordination number = 6),[33] increases the ligand rigidity, and offers sites distant from the coordination sites for future functionalization. Benzyl units were chosen to increase steric bulk and lipophilicity and therefore reduce access of competitors to the Ga^{3+} ion. The benzyl units also afforded a UV-active tag to aid in monitoring synthesis and purification.

Upon investigation of this system, we demonstrated that a species with a hydroxide anion coordinated to the Ga^{3+} center was present when the complex was formed under neutral conditions. We have shown *via* computational studies that the coordination of a hydroxide anion to the Ga^{3+} center of Ga-**Bn_2DT3A** results in a system with a larger energy barrier to dissociation than the equivalent water complex. This is reflected in the *in vitro* stability to FBS where the hydroxide complex is stable for over 2 h.

■ RESULTS AND DISCUSSION

Ligand Synthesis and Ga^{3+} Complexation. **Bn_2DT3A** was prepared in a three-step synthesis (Scheme 1), with an overall yield of 23%. Diethylenetriamine was selectively protected at the terminal amine sites through a reductive amination with benzaldehyde.[34] This selective protection is confirmed by the symmetry of the benzyl arms and alkyl backbone in the ^{1}H NMR (Figure S2). Alkylation with *tert*-butyl bromoacetate introduced protected carboxylic acid moieties to yield the proligand, **3**.[35] The incorporation of the acetate arms in two different environments can be seen in the ^{1}H NMR, reflecting the central and terminal amine functionalities (Figure S6). The proligand was then deprotected using trifluoroacetic acid to yield the ligand **Bn_2DT3A** as a white powder. The benzyl units are retained, and the two acetate arm environments are distinguishable in the ^{1}H NMR with the central arm being more shielded than the terminal arms (Figure S10).

https://doi.org/10.1021/acs.inorgchem.2c01992
Inorg. Chem. 2022, 61, 17059−17067

Complexation of Ga^{3+} by **Bn_2DT3A** was achieved at room temperature and confirmed by HRMS (m/z = 524.1734, calculated m/z = 524.1307). The ^{1}H NMR indicates a high level of asymmetry with multiple overlapping peaks with a high degree of ^{1}H−^{1}H coupling, limiting the analysis (Figure S14). Regardless, the spectra confirm the suggested model as well-resolved spectra were obtained in the pH region in which [M(L)] is the dominant species present in solution. At pD 3.3, the presence of two sharp peaks, at 3.56 and 3.85 ppm, seem to correspond to the formation of the protonated species, $[Ga(HL)]^+$, although this could not be confirmed due to overlap with the surrounding peaks. While there are clearly changes in the spectra between pD 4.0 and pD 7.3, such as the broadening of the signal between 3.45 and 3.33 ppm and the change in spectral form at 3.06 ppm, these are difficult to quantify due to the large number of overlapping signals, making precise analysis unsuitable. Hydroxide coordination leads to significant signal broadening in spectra collected above pD 6.8, which could be ascribed to intermediate ligand flexibility of the partly coordinated ligand molecule. In addition, decomplexation can be seen at high pH by the improved resolution of the ^{1}H NMR spectrum reflecting the free ligand being produced, increasing symmetry and flexibility resulting in sharp, well-defined peaks being observed at pD 8.8 and 10.0 (Figure S18).

Crystal Structure. A crystal of suitable quality for single-crystal X-ray diffraction was obtained from an acidic aqueous solution of [Ga(**Bn_2DT3A**)]. The obtained structure (Figure 1) shows a hexadentate ligand, fully satisfying the coordination

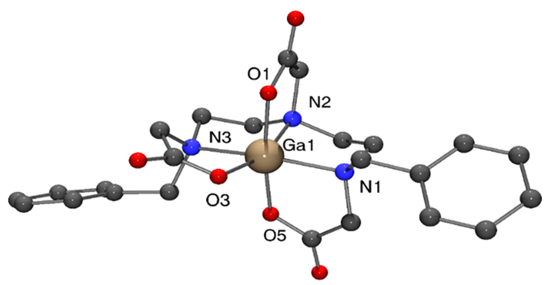

Figure 1. Molecular structure of [Ga(**Bn_2DT3A**)] determined by X-ray crystallography. Hydrogen atoms have been omitted for clarity. Colors: gallium (pale brown); carbon (gray); nitrogen (blue); oxygen (red).

sphere of Ga^{3+}. The nitrogen atoms coordinate Ga^{3+} in a *mer* fashion, as do the oxygen atoms of the carboxylate arms. The Ga^{3+} ion lies 0.220(5) Å above the plane of the three nitrogen atoms. The bite angle of each chelating unit is between 80.9(3)° and 87.0(3)°. These angles are comparable to those reported for [Ga(**DOTA**)]$^-$,[36] [Ga(**NOTA**)],[37] and [Ga(**EDTA**)]$^-$ (**EDTA** = ethylenediamine-*N*,*N*,*N*′,*N*′-tetraacetic acid, Figure S1).[38] The face where the two terminal ends of the ligand meet is slightly open in comparison to the other faces of the distorted octahedral geometry; the angle between N1 and O3 is 108.8(1)°. There is also a degree of asymmetry in the O-Ga-O angles (O1-Ga-O3 = 87.1(3)°, O3-Ga-O5 = 99.4(3)°) that is not seen in the crystal structures of the macrocyclic Ga^{3+} complexes but was also reported for [Ga(**EDTA**)]$^-$.[38] The Ga1−N2 bond length (2.077(6) Å) is a little shorter than those to N1 and N3 (2.120(7) and 2.129(8) Å, respectively). This may reflect the strain induced by coordination of the central amine to Ga^{3+}; this strain has previously been reported to prevent the coordination of the central amine in tripodal chelates with Ga^{3+}.[19,39] The gallium-to-oxygen bond lengths are shorter and lie in the range 1.937(5) to 1.987(5) Å, comparable to those reported for [Ga(**DOTA**)]$^-$,[36] [Ga(**NOTA**)],[37] and [Ga(**EDTA**)]$^-$.[38] The Ga^{3+} complex does not form any classical hydrogen bonds, but within the solid-state structure, there are many C−H···O interactions. Further details of the crystal structure determination are given in the SI (Figure S24 and Table S2). Crystals were grown at two further pH levels (5.3 and 6.8): the crystal structure obtained from these two preparations was the same; the same molecule, [Ga(**Bn_2DT3A**)], was present as a more complicated hydrate. This is likely due to the low solubility of the neutral complex in comparison to other species in solution. Further details are given in the SI (Figures S25 and S26, Table S3).

Thermodynamic Stability. Potentiometry was performed to obtain protonation constants of **Bn_2DT3A** and on the system with Ga^{3+}, Cu^{2+}, and Zn^{2+} to obtain thermodynamic stability constants and an understanding of the effect of pH on speciation in solution. Five protonation constants were determined for **Bn_2DT3A** (Table 1). By comparison to similar

Table 1. Protonation Constants of the Discussed Ligands

constant	Bn_2DT3A[a]	1[41]	DTPA[40,41]	NOTA[44,45,48]
log K_1	9.70	9.84	10.52	13.17
log K_2	7.48	9.02	8.56	5.74
log K_3	3.34	4.25	4.31	3.22
log K_4	1.50		2.8	1.96
log K_5	1.40		2.22	0.7

[a] T = 25 °C, I = 0.1 M NMe_4Cl.

ligands (Table 1),[40−45] the first three protonation constants were assigned to the amines of **Bn_2DT3A**. The remaining two protonation constants correspond to the carboxylic acid arms, with the final arm being too acidic to detect the corresponding constant. The amine sites are more acidic than those reported for **DTPA** — this is due to the stabilizing effect of the additional negatively charged carboxylate arms in **DTPA**, making amine deprotonation more difficult.[40] This can be seen by comparing the reported values for the protonation constants of glycine (log K_a = 9.8)[46] and benzylamine (log K_a = 9.36).[47] Benzylamine has a more acidic amine than glycine as it lacks the internal hydrogen bonding provided by the carboxylate arm. The two carboxylate protonation constants obtained for **Bn_2DT3A** have similar values—this contrasts with those reported for **NOTA**, which have significantly differing values. This is likely due to the flexibility of the linear ligand **Bn_2DT3A** allowing for independent protonation of the arms, whereas in the rigid macrocyclic system of **NOTA**, the arms will likely interact, forming internal hydrogen bonds where a deprotonated arm stabilizes a protonated arm at low pH. It is surprising that the carboxylate arms of **Bn_2DT3A** are approximately one log K_a unit more acidic than those of **DTPA**, although this may again be due to hydrogen bonding between the additional carboxylate arms of **DTPA**, stabilizing the partially deprotonated ligand at low pH.[40]

A 1:1 metal:ligand complex is formed between Ga^{3+} and **Bn_2DT3A** between pH 2 and 8. Above this pH, the formation of $[Ga(OH)_4]^-$ dominates the speciation of Ga^{3+} in solution.

The ligand **Bn_2DT3A** has a slightly greater affinity for Cu^{2+} than Ga^{3+} (Table 2); the affinity for both ions is greater than

https://doi.org/10.1021/acs.inorgchem.2c01992
Inorg. Chem. 2022, 61, 17059−17067

Table 2. Stability Constants and Dissociation Constants (log β_{HLM}) of Bn_2DT3A Complexes[a]

equilibrium	Ga^{3+}	Cu^{2+}	Zn^{2+}
M + L ↔ [M(L)]	18.25	18.9	14.12
[M(HL)] ↔ [M(L)] + H	2.73	2.8	4.16
[M(L)] + H_2O ↔ [M(L)(OH)] + H	5.32		12.06
[M(L)(OH)] + H_2O ↔ [M(L)$(OH)_2$] + H	8.21		

[a]Charges are omitted. (T = 25 °C, I = 0.1 M NMe_4Cl). The stability constants corresponding to the formation of [Cu(HL)] were determined without ionic strength control.

that for Zn^{2+}. The thermodynamic stability of the [Ga(**Bn_2DT3A**)] (log K[Ga(**Bn_2DT3A**)] = 18.25, p[Ga$(OH)_4$] = 5.78, Table S5) complex is lower than that of the similar systems [Ga(**DTPA**)]$^{2-}$ (log K[Ga(**DTPA**)] = 25.11, p[Ga$(OH)_4$] = 9.28, Table S5)[40,41] and [Ga(**NOTA**)] (log K[Ga(**NOTA**)] = 29.60, p[Ga$(OH)_4$] = 11.82, Table S5).[44] This is unsurprising in the case of the **NOTA** complex due to the macrocyclic nature of **NOTA**, resulting in improved thermodynamic stability due to pre-organization of the ligand prior to complexation. The difference between [Ga(**Bn_2DT3A**)] and [Ga(**DTPA**)]$^{2-}$ is more surprising (Figure 2, Table 2, Figure S46, and Table S4)—both ligands likely bind Ga^{3+} in a N_3O_3 manner. However, this can be rationalized by considering the ligand basicity; each basic site of **DTPA** is more basic than the equivalent one of **Bn_2DT3A**. This increased basicity is expected to result in an increase in stability of the formed complex.[44]

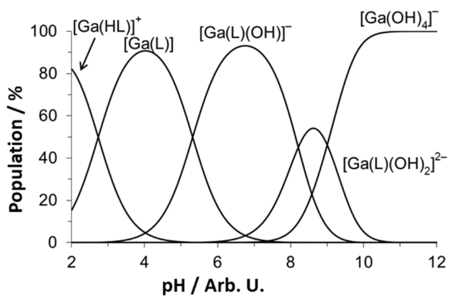

Figure 2. Speciation of Ga^{3+} in solution with **Bn_2DT3A**. (T = 25 °C, I = 0.1 M NMe_4Cl, [**Bn_2DT3A**] = 4 mM, [Ga^{3+}] = 2 mM).

As has previously been reported for the [Ga(**Dpaa**)(H_2O)] system (**Dpaa** = 6,6′-{[(carboxymethyl)azanediyl]bis(methylene)}dipicolinic acid, Figure S1), a deprotonation event occurs in the mildly acidic region (pK_a = 5.32, Figure 2).[19,39] In the case of [Ga(**Dpaa**)(H_2O)], a coordinated water molecule is the likely site of deprotonation. In the case of [Ga(**Bn_2DT3A**)], there is no evidence for a coordinated water molecule in the neutral species. As the ligand is fully deprotonated in the [Ga(**Bn_2DT3A**)] species, this additional deprotonation may be due to coordination of a hydroxide anion to the Ga^{3+} center, replacing one of the donor atoms of the ligand.[49] A similar exchange has been reported for **PIDAZTA** ligands with Ga^{3+} in which a carboxylate arm is displaced by a hydroxide (pK_a 3.75−4.04).[50]

The Ga-**Bn_2DT3A** and Ga-**DTPA** distribution diagrams (Figure 2 and Figure S46)[40,41] show identical species present in solution; however, the pH at which protonated and hydroxide species form differs. The protonated species of Ga-**DTPA** forms at a higher pH (log K = 4.06)[40,41] than that of Ga-**Bn_2DT3A** (log K = 2.73)—this is likely due to the presence of additional carboxylates resulting in easier protonation in acidic solution. In the case of Ga-**Bn_2DT3A**, this [Ga(HL)] species is likely to be due to protonation of a carboxylate arm, which as a result, is no longer coordinated to the Ga^{3+} center. A similar result is seen in the hydroxide species—the Ga-**DTPA** system forms this product at a higher pH (log K = 7.01)[40,41] than the Ga-**Bn_2DT3A** system (log K = 5.32); this is likely due to the presence of uncoordinated, charged deprotonated carboxylates resulting in a higher resistance to hydroxide attack in alkaline solution. The hydroxide species formed are likely the result of coordination of a hydroxide anion to the Ga^{3+} center with an associated

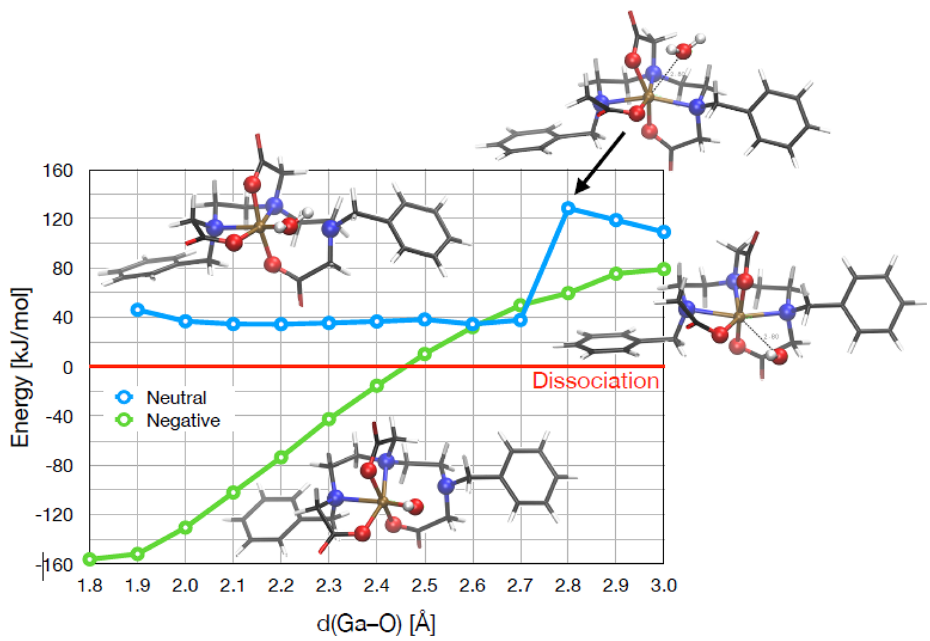

Figure 3. Calculated energy of water molecule (blue) and hydroxide anion (green) interacting with [Ga(**Bn_2DT3A**)] at various Ga−O distances.

https://doi.org/10.1021/acs.inorgchem.2c01992
Inorg. Chem. 2022, 61, 17059−17067

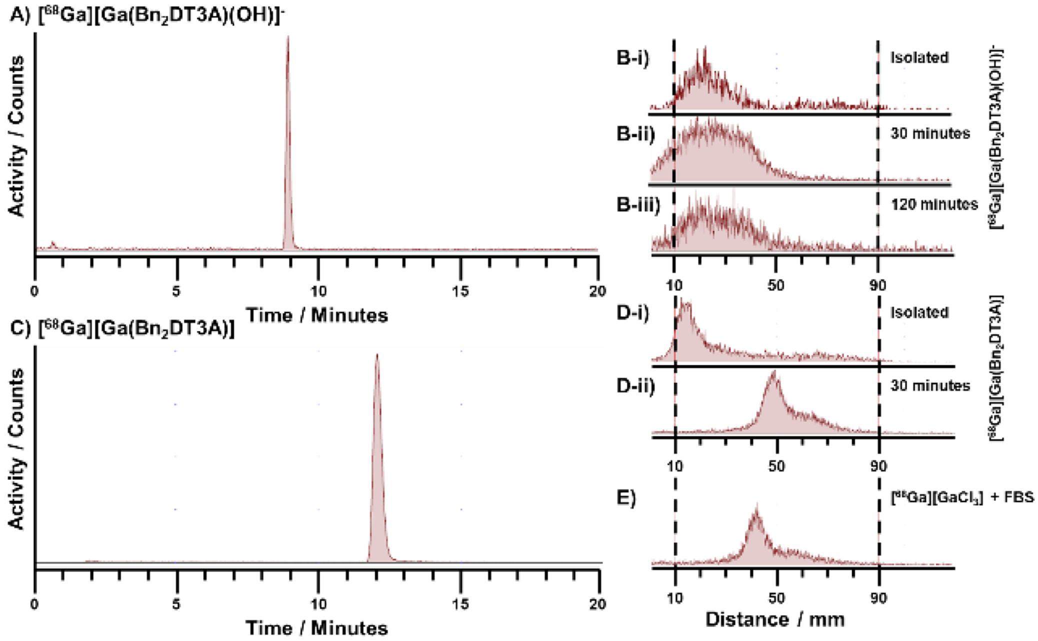

Figure 4. (A) Radio-HPLC of $[^{68}Ga][Ga(\mathbf{Bn_2DT3A})(OH)]^-$ following semipreparative HPLC purification. (B) Stability of $[^{68}Ga][Ga(\mathbf{Bn_2DT3A})(OH)]^-$ to FBS assessed by radio-TLC. (i) Isolated species. (ii) After 30 min incubation in FBS. (iii) After 120 min incubation. (C) Radio-HPLC of $[^{68}Ga][Ga(\mathbf{Bn_2DT3A})]$ following semipreparative HPLC purification. (D) Stability of $[^{68}Ga][Ga(\mathbf{Bn_2DT3A})]$ to FBS assessed by radio-TLC. (i) Isolated species. (ii) After 30 min incubation in FBS. (E) Radio-TLC of $[^{68}Ga][GaCl_3]$ incubated with FBS.

dissociation of one of the ligand coordinating atoms, either an amine or a carboxylate.

The distribution diagram clearly shows that the hydroxide species is the major species at physiological pH and is relevant for *in vitro* and *in vivo* investigations (see below).

Molecular Modeling. HF-3c calculations show that coordination of a water molecule to the $[Ga(\mathbf{Bn_2DT3A})]$ complex is not thermodynamically favorable (Figure 3). An initial energy barrier of 20 kJ mol^{-1} prevents the water molecule from approaching the Ga^{3+} ion, and, if it were to coordinate to the metal ion, the resulting species is 40 kJ mol^{-1} less stable than the dissociated system. In contrast, a hydroxide ion is shown to be able to approach the Ga^{3+} center, with an overall stabilization of 240 kJ mol^{-1} as it approaches from 3.0 to 1.8 Å. The hydroxide complex is calculated to be 160 kJ mol^{-1} more stable than the dissociated system. The calculations suggest that one of the terminal amine groups is replaced by a hydroxide anion. As the hydroxide coordination can only proceed at sufficient hydroxide anion concentration, the reaction takes place in solution with neutral pH.

Radiolabeling with ^{68}Ga. When incubated with ^{68}Ga, **Bn$_2$DT3A** was found to be capable of achieving high radiochemical yields at both pH 4 and pH 7.4; however, multiple products were formed with pH-dependent abundance. The two radiolabeled products were isolated by semi-preparative HPLC (Figure 4) and assessed independently for their stability to fetal bovine serum (FBS, Figure 4). The major product at pH 4, $[^{68}Ga][Ga(\mathbf{Bn_2DT3A})]$, was found to be poorly stable to competition by FBS, with none of the complex remaining after 30 min (Figure 4D). In contrast, the major product at pH 7.4, attributed to $[^{68}Ga][Ga(\mathbf{Bn_2DT3A})(OH)]^-$, was shown to be stable to FBS for over 2 h with no decomplexation seen (Figure 4B and Figure S20). Thus, this radiolabeled product is suitable for further PET applications.

The effect of pH on the population of the products was further investigated (Figure 5A). At low pH, a negligible

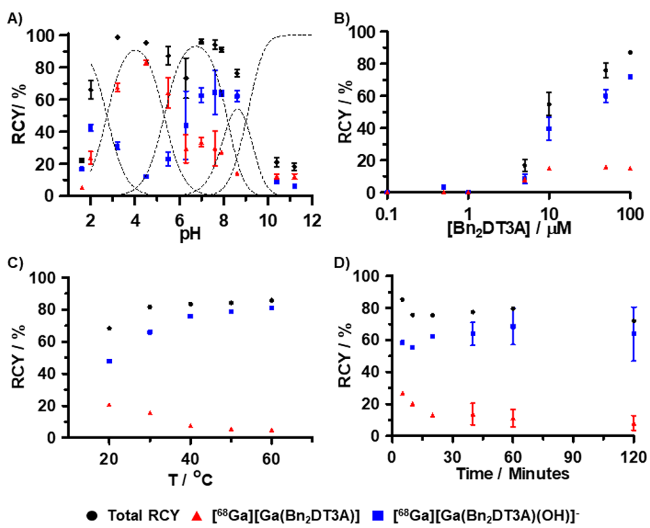

Figure 5. Effect of common reaction parameters on the radiolabeled products of $[^{68}Ga][GaCl_3]$ and **Bn$_2$DT3A** as assessed by radio-HPLC. (A) Effect of pH. [**Bn$_2$DT3A**] = 100 μM. T = 25 °C. I = 0.1 M $Na_xH_{3-x}PO_4$. t = 15 min. (B) Effect of ligand concentration. T = 25 °C. I = PBS. pH = 7.4. t = 15 min. (C) Effect of temperature. [**Bn$_2$DT3A**] = 100 μM. I = PBS. pH = 7.4. t = 5 min. (D) Effect of reaction time. [**Bn$_2$DT3A**] = 100 μM. T = 25 °C. I = PBS. pH = 7.4.

amount of the desired hydroxido species was formed; above pH 5, the FBS stable product became more populous. According to the distribution diagram, this stable product corresponds to the species $[Ga(\mathbf{Bn_2DT3A})(OH)]^-$ (Figure 5A). This is also supported by its shorter retention time when analyzed by HPLC (Figure 4A), suggesting an increased hydrophilicity due to its charge. The partition coefficient for

https://doi.org/10.1021/acs.inorgchem.2c01992
Inorg. Chem. 2022, 61, 17059−17067

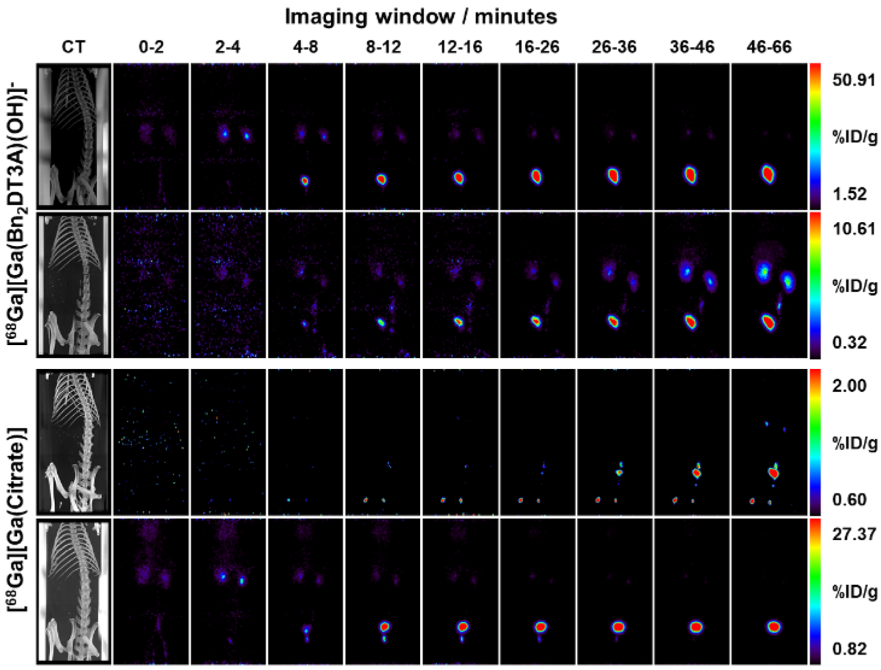

Figure 6. PET scans of healthy Sprague-Dawley rats injected with either $[^{68}Ga][Ga(\mathbf{Bn_2DT3A})(OH)]^-$ (top two rows) or $[^{68}Ga][Ga(\mathbf{Citrate})]^-$ (bottom two rows) at indicated time points. Subsequent CT scan provided for co-registration of signal.

this species was determined to be log $D_{octanol/PBS}$(pH 7.4) = −2.91 +/− 0.07, this fulfills drug development requirements, which is advantageous to future uses as a radiotracer.

The temperature of the radiolabeling reaction and the concentration of the chelator have previously been shown to affect the ratio of diastereomers formed when radiolabeling **HBED** with ^{68}Ga;[22,26] as such, these parameters were also investigated, along with the radiolabeling incubation time. The ligand concentration has a significant impact on the radiochemical yield (RCY); ligand concentrations of at least 100 μM are required to achieve RCYs >90% at pH 7.4 at room temperature in 15 min. The use of a higher ligand concentration in the radiolabeling reaction also promoted the formation of $[^{68}Ga][Ga(\mathbf{Bn_2DT3A})(OH)]^-$ (Figure 5B).

The temperature of the radiolabeling reaction has a profound impact upon the ratio of the species formed (Figure 5C); elevated temperatures favor the formation of the $[Ga(\mathbf{Bn_2DT3A})(OH)]^-$ product with ratios of 20:1 achievable at pH 7.4 and 60 °C after 5 min (Figure S21).

The reaction time has a modest effect on the RCY and the ratio of the species (Figure 5D). The increase in the ratio of species formed with increasing reaction time suggests that there is some slow exchange between the two species; this was not observed when isolating the species by semipreparative HPLC so it may require excess ligand to be present.

The obtained thermodynamic stability constants, HF-3c calculations, and kinetic inertness toward FBS all support the formation of a stable complex in which Ga^{3+} is coordinated by **$\mathbf{Bn_2DT3A}$** in a five-coordinate manner with the additional coordination site occupied by a hydroxide anion. The formation of this species, $[Ga(\mathbf{Bn_2DT3A})(OH)]^-$, occurs only in a significant proportion at pH > 5.

These optimized conditions for the production of $[^{68}Ga][Ga(\mathbf{Bn_2DT3A})(OH)]^-$ ($[L]$ > 100 μM, T > 60 °C, t > 15 min, pH 7.4) are similar to typical radiolabeling conditions for **DTPA** ($[L]$ = 155 μM, T = 25 °C, t = 20 min, pH = 3.5 or $[L]$ = 62 μM, T = 80 °C, t = 20 min, pH = 3.5)[29,30] and **CHX-A″-DTPA** ($[L]$ = 74 μM, T = 95 °C, t = 5 min, pH = 3.6−4).[32] The most noticeable difference is the increased pH of radiolabeling, potentially allowing for the radiolabeling of pH-sensitive motifs with $^{68}Ga^{3+}$ by using **$\mathbf{Bn_2DT3A}$** as a chelator instead of **DTPA** or **CHX-A″-DTPA**. In terms of stability, less than 60% $[^{68}Ga][Ga(\mathbf{DTPA})]$ remained intact after 2 h incubation in serum,[31] and $[^{68}Ga][Ga($**CHX-A″-DTPA**$)]$ was approximately 85% intact after 2 h[31]—in this comparison, $[^{68}Ga][Ga(\mathbf{Bn_2DT3A})(OH)]^-$ shows a significant improvement with no decomplexation seen after 2 h incubation with serum. Despite these differences, **$\mathbf{Bn_2DT3A}$** is still outperformed by the macrocyclic **NOTA**, which is typically radiolabeled at room temperature at much lower ligand concentrations, albeit at acidic pH ($[L]$ = 10 μM, T = 25 °C, t = 10 min, pH = 3.5).[20]

***In Vivo* Assessment.** Following optimization of the radiolabeling conditions, the $[^{68}Ga][Ga(\mathbf{Bn_2DT3A})(OH)]^-$ complex was investigated *in vivo*. Following semipreparative HPLC purification, the isolated species was reformulated into phosphate buffered saline (PBS) and administered into healthy male Sprague−Dawley rats *via* tail−vein injection. The biodistribution was monitored by sequential PET scans (Figure 6 and Figures S35−S45) followed by a computed tomography (CT) scan to allow for co-registration of the images. The activity rapidly accumulated within the kidneys before passing through the bladder, indicating a renal clearance. No uptake in the liver, lungs, or bones could be observed. When $[^{68}Ga][Ga(\mathbf{citrate})]^-$, a weakly coordinated system in which release of $[^{68}Ga][Ga^{3+}]$ is expected,[51] was studied in the same manner, some minor uptake in the lungs and transient localization in the prostate gland of the rats was observed (Figure 6 and Figures S27−S34). Uptake was also observed in the leg joints following injection of $[^{68}Ga][Ga(\mathbf{citrate})]^-$ (Figure 6), which was not observed following injection of $[^{68}Ga][Ga(\mathbf{Bn_2DT3A})(OH)]^-$. When nonchelated $[^{68}Ga][Ga^{3+}]$ is injected, high initial uptake is reported in the heart and blood followed by renal clearance with a

https://doi.org/10.1021/acs.inorgchem.2c01992
Inorg. Chem. 2022, 61, 17059−17067

prolonged heart and blood uptake along with liver and joint uptake.[51,52] In comparison to these two systems, it is clear that $[^{68}Ga][Ga(\mathbf{Bn_2DT3A})(OH)]^-$ is rapidly excreted *via* the kidneys with minimal uptake outside of this pathway, suggesting that the $^{68}Ga^{3+}$ ion remains complexed by **Bn_2DT3A**.

The rapid clearance of $[^{68}Ga][Ga(\mathbf{Bn_2DT3A})(OH)]^-$ suggests that it will be a good choice of chelate for ^{68}Ga PET when conjugated to a targeting moiety. This fast excretion will allow for rapid washout of off-target activity, which will improve the signal-to-noise ratio of the tissues of interest. The biodistribution of a targeted probe incorporating $[^{68}Ga][Ga(\mathbf{Bn_2DT3A})(OH)]^-$ should be dominated by the targeting motif as no uptake of $[^{68}Ga][Ga(\mathbf{Bn_2DT3A})(OH)]^-$ in tissues outside of the excretion pathway was observed.

Further development of the system and of bifunctional derivatives could produce a system that can be efficiently labeled at pH 7.4 without heating, resulting in a serum stable product for *in vivo* application.

■ CONCLUSIONS

A novel hexadentate chelator, **Bn_2DT3A**, has been prepared and applied to the coordination of Ga^{3+} and to radiochemistry with ^{68}Ga.

Bn_2DT3A forms a distorted octahedral *mer-mer* 1:1 complex with Ga^{3+} under acidic conditions with a thermodynamic stability of log $K[Ga(\mathbf{Bn_2DT3A})]$ = 18.25. Hydroxide anion coordination occurs with a pK_a of 5.32. HF-3c calculations attribute the species structure to the dissociation of one of the amines and insertion of a hydroxide anion.

Bn_2DT3A is capable of complexing other metal ions, as evidenced by its acceptable Cu^{2+} and Zn^{2+} thermodynamic stability constants. This gives the system a greater versatility, and this is being explored through $^{64}Cu^{2+}$ labeling experiments. While this versatility is often undesired in the design of chelators for radiometals due to the potential for complexation of other metal ions that may be present in the radiolabeling solution, the design of the ligand **Bn_2DT3A**, with benzyl units that can be substituted to increase or decrease steric hinderance and electronic properties, will allow for optimization of the system to improve selectivity for $^{68}Ga^{3+}$ in the future.

When **Bn_2DT3A** is radiolabeled with ^{68}Ga, two species are formed in a pH-dependent manner. The radiolabeling conditions can be tuned to vary the ratio of these products, and they can be isolated by semipreparative HPLC. The product that is formed above pH 5 and promoted by elevated temperatures and high ligand concentrations was attributed to the deprotonated species $[^{68}Ga][Ga(\mathbf{Bn_2DT3A})(OH)]^-$. This species was stable to biological competitors for over 2 h in contrast to the neutral species. $[^{68}Ga][Ga(\mathbf{Bn_2DT3A})(OH)]^-$ was administered to healthy rats and found to have a rapid renal clearance with negligible uptake outside of the clearance pathway.

$[Ga(\mathbf{Bn_2DT3A})]$ shows an increased *in vitro* stability upon hydroxide coordination, which allows it to be used for PET applications. This system is promising for further development of chelators for the complexation of ^{68}Ga under mild conditions.

■ ASSOCIATED CONTENT

Supporting Information

The Supporting Information is available free of charge at https://pubs.acs.org/doi/10.1021/acs.inorgchem.2c01992.

Experimental details, spectra, speciation diagrams, *in vivo* data, and crystallographic data (CCDC 1864389, 2125953) (PDF)

Accession Codes

CCDC 1864389 and 2125953 contain the supplementary crystallographic data for this paper. These data can be obtained free of charge via www.ccdc.cam.ac.uk/data_request/cif, or by emailing data_request@ccdc.cam.ac.uk, or by contacting The Cambridge Crystallographic Data Centre, 12 Union Road, Cambridge CB2 1EZ, UK; fax: +44 1223 336033.

■ AUTHOR INFORMATION

Corresponding Author

Graeme J. Stasiuk − *Department of Imaging Chemistry and Biology, School of Biomedical Engineering and Imaging Sciences, King's College London, London SE1 7EH, U.K.;* orcid.org/0000-0002-0076-2246; Email: graeme.stasiuk@kcl.ac.uk

Authors

Thomas W. Price − *Department of Imaging Chemistry and Biology, School of Biomedical Engineering and Imaging Sciences, King's College London, London SE1 7EH, U.K.; Department of Biomedical Sciences and Positron Emission Tomography Research Center, University of Hull, Hull HU6 7RX, U.K.*

Isaline Renard − *Department of Biomedical Sciences and Positron Emission Tomography Research Center, University of Hull, Hull HU6 7RX, U.K.*

Timothy J. Prior − *Chemistry, University of Hull, Hull HU6 7RX, U.K.;* orcid.org/0000-0002-7705-2701

Vojtěch Kubíček − *Department of Inorganic Chemistry, Faculty of Science, Charles University, 2030 Prague 2, Czech Republic;* orcid.org/0000-0003-0171-5713

David M. Benoit − *E.A. Milne Centre for Astrophysics, Department of Physics and Mathematics, University of Hull, Hull HU6 7RX, U.K.;* orcid.org/0000-0002-7773-6863

Stephen J. Archibald − *Department of Biomedical Sciences and Positron Emission Tomography Research Center, University of Hull, Hull HU6 7RX, U.K.;* orcid.org/0000-0001-7581-8817

Anne-Marie Seymour − *Department of Biomedical Sciences, University of Hull, Hull HU6 7RX, U.K.*

Petr Hermann − *Department of Inorganic Chemistry, Faculty of Science, Charles University, 2030 Prague 2, Czech Republic;* orcid.org/0000-0001-6250-5125

Complete contact information is available at: https://pubs.acs.org/10.1021/acs.inorgchem.2c01992

Author Contributions

T.W.P. performed the synthesis, radiolabeling, analysis of *in vivo* data, and manuscript preparation. I.R. contributed to acquisition of *in vivo* data. S.J.A. and A.-M.S. contributed to the planning and performing of *in vivo* experiments. T.J.P. contributed to the crystal structure data collection and analysis. V.K. and P.H. contributed to the potentiometric data collection and analysis. D.M.B. contributed to the molecular modeling. G.J.S. contributed to the conceptualization, super-

https://doi.org/10.1021/acs.inorgchem.2c01992
Inorg. Chem. 2022, 61, 17059−17067

vision, and funding acquisition. All authors contributed to manuscript review and editing.

Funding

The authors would like to acknowledge the Royal Society (grant RG160156) and Ministry of Education of the Czech Republic (LTC20044) for funding of this work. G.J.S. would like to thank the MRC (MR/T002573/1) and the EPSRC (EP/V027549/1 and EP/T026367/1) for funding this work.

Notes

The authors declare no competing financial interest.

■ ACKNOWLEDGMENTS

The authors would like to thank Dr. Kevin Welham and Dean Moore of the University of Hull Mass Spectrometry service for conducting the HRMS measurements and Dr. Juozas Domarkas for useful discussions. We acknowledge the Viper High Performance Computing facility of the University of Hull and its support team. We are grateful to STOE & Cie GmbH (Darmstadt, Germany) for single-crystal X-ray diffraction data collection and processing. We thank the EPSRC UK National Crystallography Service at the University of Southampton for the collection of the crystallographic data.[53]

■ REFERENCES

(1) Basu, S.; Kwee, T. C.; Surti, S.; Akin, E. A.; Yoo, D.; Alavi, A. Fundamentals of PET and PET/CT Imaging. *Ann. N. Y. Acad. Sci.* **2011**, *1228*, 1−18.

(2) Jackson, J. A.; Hungnes, I. N.; Ma, M. T.; Rivas, C. Bioconjugates of Chelators with Peptides and Proteins in Nuclear Medicine: Historical Importance, Current Innovations and Future Challenges. *Bioconjugate Chem.* **2020**, *31*, 483−491.

(3) Bartholomä, M. D.; Louie, A. S.; Valliant, J. F.; Zubieta, J. Technetium and Gallium Derived Radiopharmaceuticals: Comparing and Contrasting the Chemistry of Two Important Radiometals for the Molecular Imaging Era. *Chem. Rev.* **2010**, *110*, 2903−2920.

(4) Velikyan, I. ^{68}Ga-Based Radiopharmaceuticals: Production and Application Relationship. *Molecules* **2015**, *20*, 12913−12943.

(5) Blower, J. E.; Cooper, M. S.; Imberti, C.; Ma, M. T.; Marshall, C.; Young, J. D.; Blower, P. J. The Radiopharmaceutical Chemistry of the Radionuclides of Gallium and Indium. In *Radiopharmaceutical Chemistry*; Lewis, J. S., Windhorst, A. D., Zeglis, B. M., Eds.; Springer, Cham: Cham, 2019; pp. 255−271, DOI: 10.1007/978-3-319-98947-1_14.

(6) Lin, M.; Waligorski, G. J.; Lepera, C. G. Production of Curie Quantities of ^{68}Ga with a Medical Cyclotron via the ^{68}Zn(p,n)^{68}Ga Reaction. *Appl. Radiat. Isot.* **2018**, *133*, 1−3.

(7) Alves, F.; Alves, V. H. P.; Do Carmo, S. J. C.; Neves, A. C. B.; Silva, M.; Abrunhosa, A. J. Production of Copper-64 and Gallium-68 with a Medical Cyclotron Using Liquid Targets. *Mod. Phys. Lett. A* **2017**, *32*, 1740013.

(8) Price, T. W.; Greenman, J.; Stasiuk, G. J. Current Advances in Ligand Design for Inorganic Positron Emission Tomography Tracers ^{68}Ga, ^{64}Cu, ^{89}Zr and ^{44}Sc. *Dalton Trans.* **2016**, *45*, 15702−15724.

(9) Dotatate, P. FDA Approves ^{18}F-Fluciclovine and ^{68}Ga-DOTATATE Products. *J. Nucl. Med.* **2016**, *57*, 9N.

(10) Deroose, C. M.; Hindié, E.; Kebebew, E.; Goichot, B.; Pacak, K.; Taïeb, D.; Imperiale, A. Molecular Imaging of Gastroenteropancreatic Neuroendocrine Tumors: Current Status and Future Directions. *J. Nucl. Med.* **2016**, *57*, 1949−1956.

(11) Afshar-Oromieh, A.; Haberkorn, U.; Eder, M.; Eisenhut, M.; Zechmann, C. M. [^{68}Ga]Gallium-Labelled PSMA Ligand as Superior PET Tracer for the Diagnosis of Prostate Cancer: Comparison with ^{18}F-FECH. *Eur. J. Nucl. Med. Mol. Imaging* **2012**, *39*, 1085−1086.

(12) Eder, M.; Neels, O.; Müller, M.; Bauder-Wüst, U.; Remde, Y.; Schäfer, M.; Hennrich, U.; Eisenhut, M.; Afshar-Oromieh, A.; Haberkorn, U.; Kopka, K. Novel Preclinical and Radiopharmaceutical Aspects of [^{68}Ga]Ga-PSMA-HBED-CC: A New PET Tracer for Imaging of Prostate Cancer. *Pharmaceuticals* **2014**, *7*, 779.

(13) Hofman, M. S.; Lawrentschuk, N.; Francis, R. J.; Tang, C.; Vela, I.; Thomas, P.; Rutherford, N.; Martin, J. M.; Frydenberg, M.; Shakher, R.; Wong, L.-M.; Taubman, K.; Lee, S. T.; Hsiao, E.; Roach, P.; Nottage, M.; Kirkwood, I.; Murphy, D. G. Prostate-Specific Membrane Antigen PET-CT in Patients with High-Risk Prostate Cancer before Curative-Intent Surgery or Radiotherapy (ProPSMA): A Prospective , Randomised , Multi-Centre Study. *The Lancet* **2020**, *395*, 1208−1216.

(14) Weineisen, M.; Schottelius, M.; Simecek, J.; Baum, R. P.; Yildiz, A.; Beykan, S.; Kulkarni, H. R.; Lassmann, M.; Klette, I.; Eiber, M.; Schwaiger, M.; Wester, H.-J. ^{68}Ga- and ^{177}Lu-Labeled PSMA I&T: Optimization of a PSMA-Targeted Theranostic Concept and First Proof-of-Concept Human Studies. *J. Nucl. Med.* **2015**, *56*, 1169−1176.

(15) Hofman, M. S.; Eu, P.; Jackson, P.; Hong, E.; Binns, D.; Iravani, A.; Murphy, D.; Mitchell, C.; Siva, S.; Hicks, R. J.; Young, J. D.; Blower, P.; Mullen, G. E. Cold Kit PSMA PET Imaging: Phase I Study of ^{68}Ga-THP-PSMA PET/CT in Patients with Prostate Cancer. *J. Nucl. Med.* **2017**, *59*, 625−631.

(16) Kostelnik, T. I.; Orvig, C. Radioactive Main Group and Rare Earth Metals for Imaging and Therapy. *Chem. Rev.* **2019**, *119*, 902−956.

(17) Notni, J.; Šimeček, J.; Hermann, P.; Wester, H.-J. TRAP, a Powerful and Versatile Framework for Gallium-68 Radiopharmaceuticals. *Chem. − Eur. J.* **2011**, *17*, 14718−14722.

(18) Ferreira, C. L.; Lamsa, E.; Woods, M.; Duan, Y.; Fernando, P.; Bensimon, C.; Kordos, M.; Guenther, K.; Jurek, P.; Kiefer, G. E. Evaluation of Bifunctional Chelates for the Development of Gallium-Based Radiopharmaceuticals. *Bioconjugate Chem.* **2010**, *21*, 531−536.

(19) Weekes, D. M.; Ramogida, C. F.; Jaraquemada-Peláez, M. D. G.; Patrick, B. O.; Apte, C.; Kostelnik, T. I.; Cawthray, J. F.; Murphy, L.; Orvig, C. Dipicolinate Complexes of Gallium(III) and Lanthanum(III). *Inorg. Chem.* **2016**, *55*, 12544−12558.

(20) Velikyan, I.; Maecke, H.; Langstrom, B. Convenient Preparation of Ga-68-Based PET-Radiopharmaceuticals at Room Temperature. *Bioconjugate Chem.* **2008**, *19*, 569−573.

(21) Blower, P. J.; Cusnir, R.; Darwesh, A.; Long, N. J.; Ma, M. T.; Osborne, B. E.; Price, T. W.; Reid, G.; Southworth, R.; Stasiuk, G. J.; Terry, S. Y. A.; de Rosales, R. T. M. *Chapter 1 - Gallium: New Developments and Applications in Radiopharmaceutics*, 1st ed.; Hubbard, C. D., van Eldik, R., Eds.; Elsevier, 2021, DOI: 10.1016/bs.adioch.2021.04.002.

(22) Tsionou, M. I.; Knapp, C. E.; Foley, C. A.; Munteanu, C. R.; Cakebread, A.; Imberti, C.; Eykyn, T. R.; Young, J. D.; Paterson, B. M.; Blower, P. J.; Ma, M. T. Comparison of Macrocyclic and Acyclic Chelators for Gallium-68 Radiolabelling. *RSC Adv.* **2017**, *7*, 49586−49599.

(23) Berry, D. J.; Ma, Y.; Ballinger, J. R.; Tavaré, R.; Koers, A.; Sunassee, K.; Zhou, T.; Nawaz, S.; Mullen, G. E. D.; Hider, R. C.; Blower, P. J. Efficient Bifunctional Gallium-68 Chelators for Positron Emission Tomography: Tris(Hydroxypyridinone) Ligands. *Chem. Commun.* **2011**, *47*, 7068−7070.

(24) Imberti, C.; Chen, Y.-L.; Foley, C. A.; Ma, M. T.; Paterson, B. M.; Wang, Y.; Young, J. D.; Hider, R. C.; Blower, P. J. Tuning the Properties of Tris(Hydroxypyridinone) Ligands: Efficient ^{68}Ga Chelators for PET Imaging. *Dalton Trans.* **2019**, *48*, 4299−4313.

(25) Seemann, J.; Waldron, B. P.; Roesch, F.; Parker, D. Approaching "kit-Type" Labelling with ^{68}Ga: The DATA Chelators. *ChemMedChem* **2015**, *10*, 1019−1026.

(26) Schuhmacher, J.; Klivényi, G.; Matys, R.; Stadler, M.; Regiert, T.; Hauser, H.; Doll, J.; Maier-Borst, W.; Zöller, M. Multistep Tumor Targeting in Nude Mice Using Bispecific Antibodies and a Gallium Chelate Suitable for Immunoscintigraphy with Positron Emission Tomography. *Cancer Res.* **1995**, *55*, 115−123.

(27) Ray Banerjee, S.; Chen, Z.; Pullambhatla, M.; Lisok, A.; Chen, J.; Mease, R. C.; Pomper, M. G. Preclinical Comparative Study of

^{68}Ga-Labeled DOTA, NOTA, and HBED-CC Chelated Radiotracers for Targeting PSMA. *Bioconjugate Chem.* **2016**, *27*, 1447−1455.

(28) Dumont, R. A.; Deininger, F.; Haubner, R.; Maecke, H. R.; Weber, W. A.; Fani, M. Novel ^{64}Cu- and ^{68}Ga-Labeled RGD Conjugates Show Improved PET Imaging of 3 Integrin Expression and Facile Radiosynthesis. *J. Nucl. Med.* **2011**, *52*, 1276−1284.

(29) Lee, J. Y.; Jeong, J. M.; Kim, Y. J.; Jeong, H. J.; Lee, Y. S.; Lee, D. S.; Chung, J. K. Preparation of Ga-68-NOTA as a Renal PET Agent and Feasibility Tests in Mice. *Nucl. Med. Biol.* **2014**, *41*, 210−215.

(30) Chakravarty, R.; Chakraborty, S.; Dash, A.; Pillai, M. R. A. Detailed Evaluation on the Effect of Metal Ion Impurities on Complexation of Generator Eluted ^{68}Ga with Different Bifunctional Chelators. *Nucl. Med. Biol.* **2013**, *40*, 197−205.

(31) Koop, B.; Reske, S. N.; Neumaier, B. Labelling of a Monoclonal Antibody with ^{68}Ga Using Three DTPA-Based Bifunctional Ligands and Their in Vitro Evaluation for Application in Radioimmunotherapy. *Radiochim. Acta* **2007**, *95*, 39−42.

(32) Wüstemann, T.; Bauder-wüst, U.; Schäfer, M.; Eder, M.; Benesova, M.; Leotta, K.; Kratochwil, C.; Haberkorn, U.; Kopka, K.; Mier, W. Design of Internalizing PSMA-Specific Glu-Ureido-Based Radiotherapeuticals. *Theranostics* **2016**, *6*, 1085−1095.

(33) Wadas, T. J.; Wong, E. H.; Weisman, G. R.; Anderson, C. J. Coordinating Radiometals of Copper, Gallium, Indium, Yttrium, and Zirconium for PET and SPECT Imaging of Disease. *Chem. Rev.* **2010**, *110*, 2858−2902.

(34) Gros, G.; Hasserodt, J. Multigram Four-Step Synthesis of 1,4,7-Triazacyclononanes with 2Ra/Rb N-Functionalization Pattern by Starting from Diethylenetriamine. *Eur. J. Org. Chem.* **2015**, *2015*, 183−87.

(35) Price, E. W.; Cawthray, J. F.; Bailey, G. A.; Ferreira, C. L.; Boros, E.; Adam, M. J.; Orvig, C. H_4octapa: An Acyclic Chelator for In-111 Radiopharmaceuticals. *J. Am. Chem. Soc.* **2012**, *134*, 8670−8683.

(36) Viola, N. A.; Rarig, R. S., Jr.; Ouellette, W.; Doyle, R. P. Synthesis, Structure and Thermal Analysis of the Gallium Complex of 1,4,7,10-Tetraazacyclo-Dodecane-N,N′,N″,N‴-Tetraacetic Acid (DOTA). *Polyhedron* **2006**, *25*, 3457−3462.

(37) Moore, D. A.; Fanwick, P. E.; Welch, M. J. A Novel Hexachelating Amino−Thiol Ligand and Its Complex with Gallium(III). *Inorg. Chem.* **1990**, *29*, 672−676.

(38) Jung, W.-S.; Chung, Y. K.; Shin, D. M.; Kim, S.-D. Crystal- and Solution-Structure Characteristics of Ethylene Diaminetetraacetatoaluminate (III) and Gallate (III). *Bull. Chem. Soc. Jpn.* **2002**, *1267*, 1263−1267.

(39) Price, T. W.; Gallo, J.; Kubíček, V.; Böhmová, Z.; Prior, T. J.; Greenman, J.; Hermann, P.; Stasiuk, G. J. Amino Acid Based Gallium-68 Chelators Capable of Radiolabeling at Neutral PH. *Dalton Trans.* **2017**, *46*, 16973−16982.

(40) Delgado, R.; Do Carmo Figueira, M.; Quintino, S.; Figueira, M. D.; Quintino, S. Redox Method for the Determination of Stability Constants of Some Trivalent Metal Complexes. *Talanta* **1997**, *45*, 451−462.

(41) National Institute of Standards and Technology: Gaithersburg, M. D. *NIST Standard Reference Database 46 (Critically Selected Stability Constants of Metal Complexes)* Version 7.0, 2003.

(42) Costa, J.; Ruloff, R.; Burai, L.; Helm, L.; Merbach, A. E. Rigid $M^{II}L_2Gd_2^{III}$ (M = Fe, Ru) Complexes of a Terpyridine-Based Heteroditopic Chelate: A Class of Candidates for MRI Contrast Agents. *J. Am. Chem. Soc.* **2005**, *127*, 5147−5157.

(43) McMurry, T. J.; Pippin, C. G.; Wu, C.; Deal, K. A.; Brechbiel, M. W.; Mirzadeh, S.; Gansow, O. A. Physical Parameters and Biological Stability of Yttrium(III) Diethylenetriaminepentaacetic Acid Derivative Conjugates. *J. Med. Chem.* **1998**, *41*, 3546−3549.

(44) Šimeček, J.; Schulz, M.; Notni, J.; Plutnar, J.; Kubíček, V.; Havlíčková, J.; Hermann, P. Complexation of Metal Ions with TRAP (1,4,7-Triazacyclononane Phosphinic Acid) Ligands and 1,4,7-Triazacyclononane-1,4,7-Triacetic Acid: Phosphinate-Containing Ligands as Unique Chelators for Trivalent Gallium. *Inorg. Chem.* **2012**, *51*, 577−590.

(45) Kubíček, V.; Böhmová, Z.; Ševčíková, R.; Vaněk, J.; Lubal, P.; Poláková, Z.; Michalicová, R.; Kotek, J.; Hermann, P. NOTA Complexes with Copper(II) and Divalent Metal Ions: Kinetic and Thermodynamic Studies. *Inorg. Chem.* **2018**, *57*, 3061−3072.

(46) Guranda, D. T.; Ushakov, G. A.; Yolkin, P. G.; Švedas, V. K. Thermodynamics of Phenylacetamides Synthesis: Linear Free Energy Relationship with the PK of Amine. *J. Mol. Catal. B: Enzym.* **2012**, *74*, 48−53.

(47) Arrowsmith, C. H.; Guo, H.-X.; Kresge, A. J. Hydrogen Isotope Fractionation Factors for Benzylamine and Benzylammonium Ion. Comparison of Fractionation Factors for Neutral and Positively-Charged Nitrogen-Hydrogen Bonds. *J. Am. Chem. Soc.* **1994**, *116*, 8890−8894.

(48) Drahoš, B.; Kubíček, V.; Bonnet, C. S.; Hermann, P.; Lukeš, I.; Tóth, É. Dissociation Kinetics of Mn^{2+} Complexes of NOTA and DOTA. *Dalton Trans.* **2011**, *40*, 1945−1951.

(49) Šimeček, J.; Zemek, O.; Hermann, P.; Notni, J.; Wester, H.-J. Tailored Gallium(III) Chelator NOPO: Synthesis, Characterization, Bioconjugation, and Application in Preclinical Ga-68-PET *Imaging. Mol. Pharmaceutics* **2014**, *11*, 3893−3903.

(50) Farkas, E.; Vágner, A.; Negri, R.; Lattuada, L.; Tóth, I.; Colombo, V.; Esteban-Gómez, D.; Platas-Iglesias, C.; Notni, J.; Baranyai, Z.; Giovenzana, G. B. PIDAZTA: Structurally Constrained Chelators for the Efficient Formation of Stable Gallium-68 Complexes at Physiological pH. *Chem. − Eur. J.* **2019**, *25*, 10698−10709.

(51) Autio, A.; Virtanen, H.; Tolvanen, T.; Liljenbäck, H.; Oikonen, V.; Saanijoki, T.; Siitonen, R.; Käkelä, M.; Schüssele, A.; Teräs, M.; Roivainen, A. Absorption, Distribution and Excretion of Intravenously Injected ^{68}Ge/^{68}Ga Generator Eluate in Healthy Rats, and Estimation of Human Radiation Dosimetry. *EJNMMI Res.* **2015**, *5*, 40.

(52) Steinberg, J. D.; Raju, A.; Chandrasekharan, P.; Yang, C.-T.; Khoo, K.; Abastado, J.-P.; Robins, E. G.; Townsend, D. W. Negative Contrast Cerenkov Luminescence Imaging of Blood Vessels in a Tumor Mouse Model Using [^{68}Ga]Gallium Chloride. *EJNMMI Res* **2014**, *4*, 15.

(53) Coles, S. J.; Gale, P. A. Changing and Challenging Times for Service Crystallography. *Chem. Sci.* **2012**, *3*, 683−689.

https://doi.org/10.1021/acs.inorgchem.2c01992
Inorg. Chem. 2022, 61, 17059−17067